Chemistry–A European Journal
Research Article
doi.org/10.1002/chem.202302002
Chemistry Europe
European Chemical Societies Publishing
www.chemeurj.org

Special Collection

Modulating Strain in Twisted Pyrene-Fused Azaacenes

Javier Mateos-Martín,[a] Kais Dhbaibi,[a] Manuel Melle-Franco,[b] and Aurelio Mateo-Alonso*[a, c]

On the occasion of Maurizio Prato's 70th birthday.

The design and synthesis of strained aromatics provide an additional insight into the relationship between structure and properties. In the last years, several approaches to twist pyrene-fused azaacenes have been developed that allow to introduce twists of different sizes. Herein, we describe the synthesis of a new set of twisted dibenzotetraazahexacenes constituted by fused pyrene and quinoxaline residues that have been distorted by introducing increasingly larger substituents on the quinoxaline residues. Their twisted structure has been demonstrated by single-crystal X-ray diffraction. Furthermore, absorption, fluorescence, electrochemical and theoretical studies shine light on the effects of the substituents and twists on the optoelectronic and redox properties.

Introduction

Twisted polycyclic aromatic hydrocarbons are receiving increasing attention due to their inherent optoelectronic and chiroptical properties.[1–16] Steric crowding has proven to be an efficient tool to introduce twists in a wide variety of aromatic systems.[1–11,17–19] Among these, pyrene-fused acenes[11,20–22] have been used as a platform for investigating the effects of such twists on the structure and properties, thanks to the availability of several approaches that allow to twist their backbone, such as phenyl,[23–25] silyl,[11,19, 26] cyanide[27] and bisimide[28] overcrowding. Given the large variety of trisubstituted silyl groups, silyl overcrowding[19,26] allows to investigate the effects of volume and rigidity. Recently, we have shown how the alignment of sterically-demanding substituents along the backbone is key to maximize the strain and in turn the twist angles in pyrene-fused acenes constituted by fused pyrene and quinoxaline residues.[19] This alignment was achieved by eliminating the acetylenes sitting on the pyrene residues (Figures 1a and b). Notably, this group alignment allowed not only to twist the backbone to a higher degree but also to correlate changes in the optoelectronic properties with the size of the twist angles. By increasing steric demand of the groups sitting directly on the pyrene residue and keeping the same silyl-ethynyl groups on the quinoxaline residues (Figure 1b), it was observed how the absorption and emission properties of highly twisted pyrene-fused azaacenes are shifted to lower energies,[19] offering a way to modulate their optoelectronic properties.

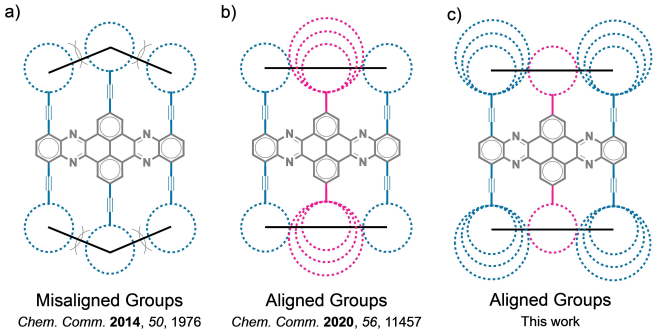

Figure 1. Pyrene-fused azaacenes with a) misaligned groups of the same size and b,c) aligned groups of different sizes at different positions.

Herein, we describe the synthesis of a new series of twisted pyrene-fused azaacenes with aligned groups that allow understanding the effects of the groups sitting on the quinoxaline residues. This new set shows increasingly larger substituents on the quinoxaline residues (Figure 1c) and provide a complete picture of the effects of substituent size, volume and rigidity on the twisted structure and on the fundamental optoelectronic and redox properties of twisted pyrene-fused azaacenes.

Results and Discussion

The synthesis of this new pyrene-fused twistacene series is achieved by cyclocondensation between pyrene-4,5,9,10-tetraone and *o*-diamine derivatives equipped with bulky groups. 2,7-Di-*tert*-butylpyrene-4,5,9,10-tetraone (**6**),[29] 2,7-di-tri-*iso*-propylsilylpyrene-

[a] *Dr. J. Mateos-Martín, Dr. K. Dhbaibi, Prof. Dr. A. Mateo-Alonso*
POLYMAT
University of the Basque Country UPV/EHU
Avenida de Tolosa 72, E-20018, Donostia-San Sebastián (Spain)
E-mail: amateo@polymat.eu
[b] *Prof. Dr. M. Melle-Franco*
CICECO – Aveiro Institute of Materials, Department of Chemistry
University of Aveiro
3810–193 Aveiro (Portugal)
[c] *Prof. Dr. A. Mateo-Alonso*
Ikerbasque
Basque Foundation for Science
Bilbao (Spain)

Supporting information for this article is available on the WWW under https://doi.org/10.1002/chem.202302002

This article is part of a joint Special Collection in honor of Maurizio Prato.

4,5,9,10-tetraone (**7**),[19] 2,7-di-triphenylsilylpyrene-4,5,9,10-tetraone (**8**),[19] 4,7-bis((tri-*iso*-propylsilyl)ethynyl)benzo-5,6-diamine (**9**),[26] and 4,7-bis((triphenylsilyl)ethynyl)benzo-5,6-diamine (**10**)[26] were prepared according to literature procedures.

The first set of dibenzotetraazahexacenes (Scheme 1) were obtained by the cyclocondensation between pyrenetetraone **6** with *tert*-butyl groups and diamines **9** and **10** with tri-*iso*-propyl (TIPS) and triphenylsilyl (TPS) groups, respectively, yielding dibenzotetraazahexacenes **1** (86%) and **2** (93%) in high yields. The second set of dibenzotetrazahexacenes (Scheme 1) was obtained by reactions between pyrenetetraone **7** equipped with TIPS substituents and diamines **9** and **10** equipped with TIPS and TPS groups, respectively. To our surprise, the reaction between **7** and **9**, both equipped with TIPS groups, failed to yield the desire double cyclocondensation product after several attempts, which included different temperatures, catalysts and solvents (Scheme S1, Table S1 and Figure S1). Instead, we observed either the formation of the monocyclocondensation product or no reaction. Even more surprising is the fact that the reaction between the same TIPS-substituted pyrenetetraone **7** and diamine **10** that is substituted with bulkier TPS groups proceeds without any problem, yielding the desired dibenzohexacene **3** (40%). The third and last set of dibenzotetrazahexacenes (Scheme 1) was obtained by reaction between pyrenetetraone **8** equipped with TPS groups and diamines **9** and **10** equipped with TIPS and TPS groups respectively, which afforded **4** (90%) and **5** (46%). A likely rationale for the successful formation of dibenzotetraazahexacenes **3**–**5** would be that the TPS groups, although bulkier and more rigid, can partially accommodate other groups in-between the phenyl substituents as illustrated by the crystal structures below. Meanwhile in the case of TIPS groups, although smaller, they cannot conformationally accommodate other TIPS groups, resulting in a higher sterical demand that might have inhibited the second cyclocondensation. The structures of dibenzotetraazahexacenes were confirmed by Nuclear Magnetic Resonance (^{1}H and ^{13}C NMR) and by Matrix Assisted Laser Desorption Ionization mass spectrometry coupled to a time-of-flight analyzer (MALDI-TOF).

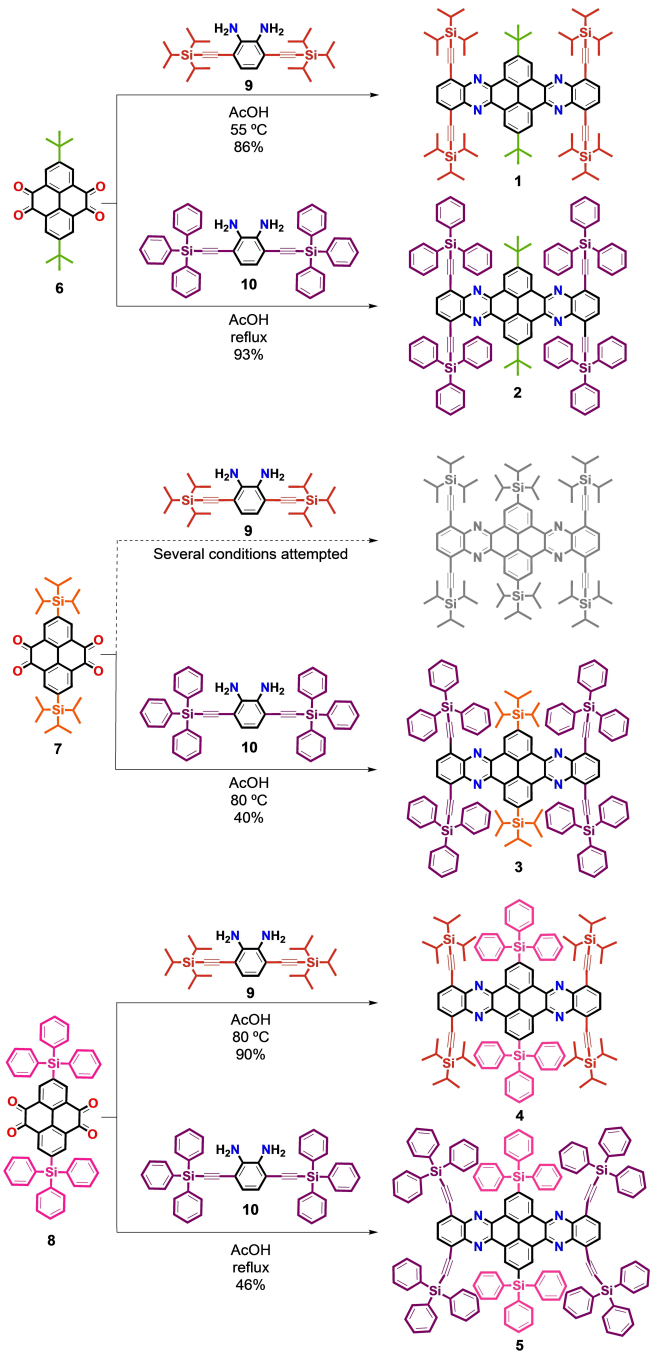

Scheme 1. Synthesis of dibenzotetraazahexacenes **1**–**5**.

Crystals suitable for X-ray diffraction were obtained for dibenzotetraazahexacenes **1**–**5** by vapor diffusion of ethanol into a toluene solution (Figure 2). The crystal structures of **2**–**5** show an evident steric interaction between groups sitting on the quinoxaline and on the pyrene residues. This interaction is evidenced by the alternate twists along the dibenzotetraaza-hexacene backbone, where the pyrene residue is out of plane, and also, by the bent acetylenes. To shine light on the effects of the different groups on the structure of the dibenzotetraazahexacenes, two different dihedral angles were compared. First, θ_{ABCD} corresponds to the end-to-center twist angle that correlates to the distortion of the core, while θ_{EFGH} corresponds to the pyrene-acetylene twist angle that correlates to the bending of the acetylene groups. Then maximum θ_{ABCD} and θ_{EFGH} values are shown in Figure 2 and are compared in terms of the increasing size of the groups sitting on the quinaxolines. In the case of compound **1** the *tert*-butyl groups do not practically interact with the TIPS groups on the quinoxaline residues as demonstrated by θ_{ABCD} and θ_{EFGH} values of 1° and 2°, respectively. On the other hand, in compound **2**, the bulkier and more rigid TPS groups on the quinoxaline residues show some steric interaction with the *tert*-butyls on the pyrene that give rise to an alternated twisted structure with 5° and 8°, respectively for θ_{ABCD} and θ_{EFGH}. In the case of **3**, the backbone is substantially more distorted with 13° and 17°, respectively for θ_{ABCD} and θ_{EFGH}, which illustrate an effective steric interaction between the larger TIPS and TPS groups. When compounds **4** and **5** that show TPS substituents in the pyrene residue are compared, we observe similar θ_{ABCD} and θ_{EFGH} values for **4** (11° and 18°, respectively) and **5** (11° and 17°, respectively) that are also similar to those of **3**.

The packing in the crystal structure varies from one dibenzohexacene to the other (Figure S2), which is expected from

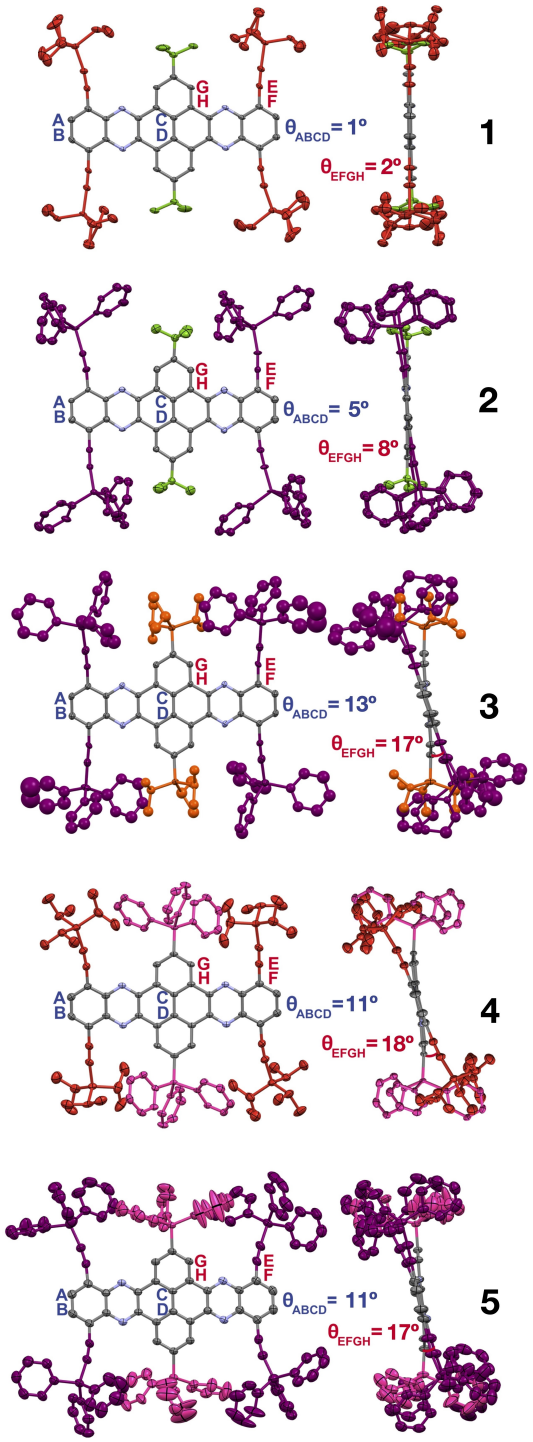

Figure 2. Crystal structures of compounds **1**–**5** showing the maximum θ_{ABCD} and θ_{EFGH} values for each structure.

the different substituents. Dibenzohexacene **1** packs in a brick-like arrangement. Dibenzohexacene **2** adopts a herringbone arrangement and crystallizes with a molecule of toluene π-stacked between the planes. Dibenzohexacenes **3** and **4** adopt a displaced columnar arrangement. In contrast, dibenzohexacene **5** presents similar packing to that observed in **1**.

The electronic absorption spectra of **1**–**5** in CH_2Cl_2 (Figures 3a–c, Table 1) show the typical ρ and ß bands observed in pyrene-fused acene systems.[30–33] By comparing different sets of molecules, we can discern the effects of the size of the substituents on the electronic absorption properties. When we compare the electronic absorption spectra of dibenzohexacenes with the same group on the pyrene residue and with varying groups on the quinoxaline residue, we observe that the absorption appears increasingly redshifted as the size of the substituents increase. For instance, the ρ band of **2** is red-shifted (4 nm) when compared to **1**. The ρ band of compound **3** is the most red-shifted of the whole series. The ρ band of **5** is also red-shifted (4 nm) when compared to **4**. These redshifts in the optoelectronic properties can be attributed to an increasingly more twisted structure in solution in agreement with previous experimental and theoretical studies that show how the absorption and emission shift to lower energies as result of increasing twists.[7,19] As such, it should be noted that twist angles in solution may differ from those in the solid-state that might be affected by packing effects. To further confirm that the observed absorption redshifts are due to the distorted aromatic core and not due to the electronic effects of the substituents, parallel absorption studies were carried out on model benzothiadiazoles substituted with either two TIPS-acetylenes or two TPS-acetylenes on the 4,7 positions (Figure S3). The measurements on the model compounds show the opposite trend, namely the absorption features of the benzothiadiazole with the TPS groups are blue-shifted in comparison to those of the benzothiadiazole with the TIPS groups.

All dibenzohexacenes are fluorescent and their fluorescence spectra were recorded in CH_2Cl_2 upon excitation at 357 nm (Figures 3a–c, Table 1). In the case of **1** and **4**, the fluorescence spectra show a broad and featureless fluorescence band, whereas, in the case of **2**, **3** and **5** the fluorescence spectra show a band with clear vibronic features. These differences are consistent with the presence of TPS-acetylene groups sitting on the quinoxaline

Table 1. Selected optoelectronic, redox, and electronic properties of **1**–**5**.

	1	2	3	4	5
λ_{max} (nm)[a]	435	439	443	437	441
λ_{em} (nm)[a]	464	464	455	478	449
φ[a,b]	0.29	0.66	0.78	0.38	0.75
$E_{1/2}^{I}$ (eV)[c]	−1.61	−1.58	−1.58	−1.64	−1.54
$E_{1/2}^{II}$ (eV)[c]	−1.83	−1.70	−1.69	−1.78	−1.65
E_{pc}^{III} (eV)[c]	−2.41	−2.26	−2.24	−2.37	−2.18
E_g (eV)[d]	2.76	2.72	2.73	2.76	2.70
E_{LUMO} (eV)[e]	−3.26	−3.34	−3.36	−3.29	−3.38
E_{HOMO} (eV)[f]	−6.02	−6.06	−6.09	−6.05	−6.08

[a] CH_2Cl_2. [b] Fluorescence quantum yield was calculated by using 9,10-diphenylanthracene as reference. [c] E vs Fc/Fc^+ in nBu_4NPF_6 in CH_2Cl_2 (0.1 M); where $E_{1/2}$ and E_{pc} denote respectively the half-wave potential and the cathodic peak potential. [d] Optical band gap calculated using equation $E_g = hc/\lambda_{onset} \approx 1240/\lambda_{onset}$ (nm); where λ_{onset} is the offset wavelength from the lowest energy absorption band. [e] $E_{LUMO} = -(E_{1/2\,(ONSET)}^{I} + 4.80$ eV); where $E_{1/2\,(ONSET)}^{I}$ is the onset potential of the first reduction wave. [f] $E_{HOMO} = E_{LUMO} - E_g$.

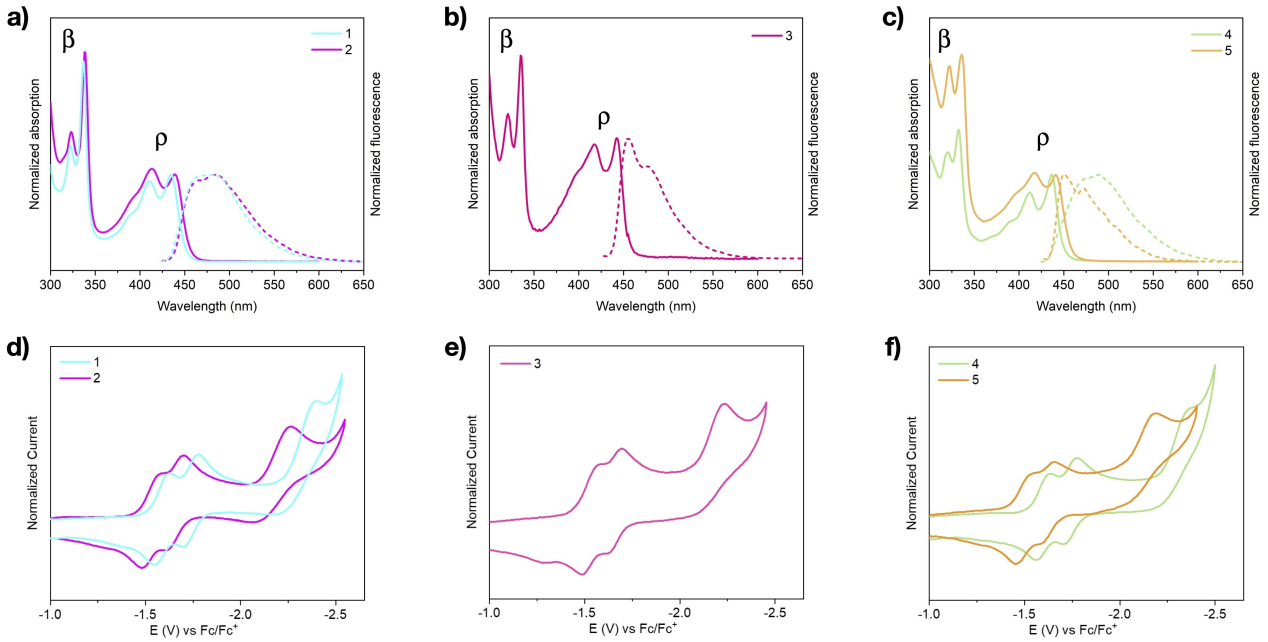

Figure 3. a-c) Normalized absorption (solid line) and fluorescence (dotted line) spectra of **1**–**5** in CH_2Cl_2. d-f) Normalized cyclic voltammograms of **1**–**5** in *n*-Bu_4NPF_6 (0.1 M) in CH_2Cl_2.

residues. To ensure that the differences in the fluorescence properties are not the result of aggregation in solution, we carried out dilution measurements (Figure S4), and also the fluorescence spectra in solution were compared with those in the solid-state (Figure S5). No evidence of aggregation was observed in solution, which is consistent with the presence of the large and bulky substituents in all cases. Similarly, the differences in the fluorescence quantum yields are consistent with substituent effects. Dibenzohexacenes **1** (0.29) and **4** (0.38) with TIPS-acetylene groups in the quinoxaline residues show the lowest quantum yields (φ), whereas **2** (0.66), **3** (0.78) and **5** (0.75) with TPS-acetylene groups in the quinoxaline residues show substantially higher quantum yields. Considering that TIPS groups are not photo- or redox active, we can rule out any electronic effects on the lower quantum yields for **1** and **4**.

The electrochemical properties of the dibenzohexacenes were investigated by cyclic voltammetry in CH_2Cl_2 using *n*-Bu_4NPF_6 0.1 M as electrolyte and the ferrocene/ferrocenium (Fc/Fc^+) couple as the internal standard. The cyclic voltammograms of **1**–**5** (Figures 3d–f, Table 1) show two reversible reduction waves with half-wave potentials ($E_{1/2}$) approximately at −1.6 and −1.8 V and one irreversible with peak potentials (E_{pc}) around −2.3 V. No oxidation processes were observed within the selected solvent-supported electrolyte window. When we compare the potentials of the dibenzohexacenes with the same group on the pyrene residue and with varying groups on the quinoxaline residue, we observe that $E_{1/2}$ become less negative as the size of the groups increases. For instance, the $E_{1/2}^{I}$, $E_{1/2}^{II}$ and E_{pc}^{III} of **2** are anodically shifted when compared to those of **1**. The $E_{1/2}^{I}$, $E_{1/2}^{II}$ and E_{pc}^{III} of **3** are very similar to those of **2**. The $E_{1/2}^{I}$, $E_{1/2}^{II}$ and E_{pc}^{III} of **5** are also anodically shifted when compared to those of **4**. These differences in the redox potentials can be attributed to the TPS groups, as the cyclic voltammograms for reference benzothiadiazoles substituted with either two TIPS-acetylenes or two TPS-acetylenes on the 4,7 positions (Figure S6) also show the more anodic potentials in the presence of TPS groups.

The HOMO-LUMO gaps (E_g) were estimated from the onset of the lowest energy absorption band are very similar in all cases. The electrochemical LUMO energies or electron affinities were estimated from the onset of the first reduction waves (Table 1). The E_{LUMO} values are in the same range as those of organic *n*-type semiconductors[34] and in the case of TPS-substituted systems, they show slightly lower values.

For a deeper understanding of the optoelectronic properties, the electronic structure of **1**–**5** was calculated by TD-DFT (B3LYP-6-31G(d,p)-CH_2Cl_2, Table S2). Negligible differences in the order of 0.01 eV are observed among the twisted systems. Notably, meanwhile virtually identical electronic densities for the different frontier orbitals are observed for **1**–**5**, in the case of **5**, the inversion of the LUMO and LUMO+1 (Figure S7) is clearly observed. This orbital inversion has been already described for other twisted pyrene-fused azaacenes once a critical twist angle has been attained.[19,26]

Conclusions

To conclude, we have described the synthesis of a series of twisted dibenzotetraazahexacenes that allow us to investigate the effect of size, volume and rigidity of the substituents sitting on the quinoxaline residues on their twisted structure and on their fundamental optoelectronic and redox properties. Dibenzotetraazahexacenes with mixed TIPS and TPS substituents provide the largest twist angles in the solid state. The redshifts observed on the electronic absorption properties can be ascribed to a larger

twist angle, which is consistent with previous observations[7,19] and with parallel studies carried out on a series of reference compounds. Whereas, the differences observed in the fluorescence and redox properties are related to the nature of the different substituents. Overall, this work shines light on the particular properties of distorted aromatics and also opens up new possibilities for the design and synthesis of other types of strained aromatics.

Supporting Information

Supporting Schemes, Tables and Figures. Full experimental procedures. Deposition Numbers 2271828 (for **1**), 2271814 (for **2**), 2271815 (for **3**), 2271817 (for **4**), 2271821 (for **5**) contain the supplementary crystallographic data for this paper. These data are provided free of charge by the joint Cambridge Crystallographic Data Centre and Fachinformationszentrum Karlsruhe Access Structures service.

Acknowledgements

This work was carried out with support from the Basque Science Foundation for Science (Ikerbasque), POLYMAT, the University of the Basque Country, Diputación de Guipúzcoa, Gobierno Vasco (PIBA_2022_1_0031 and BERC programme) and Gobierno de España (Projects PID2021-124484OB-I00 and CEX2020-001067-M financed by MCIN/AEI/10.13039/501100011033). Project (PCI2022-132921) funded by the Agencia Estatal de Investigación through the PCI 2022 and M-ERA.NET 2021 calls. This project has received funding from the European Research Council (ERC) under the European Union's Horizon2020 research and innovation programme (Grant Agreement No. 722951). This work was funded by the European Union under the Horizon Europe grant 101046231. Technical and human support provided by SGIker of UPV/EHU and European funding (ERDF and ESF) is acknowledged. In addition, support through the project IF/00894/2015, the advanced computing project 2021.09622.CPCA granting access to the Navigator cluster at LCA-UC, and within the scope of the project CICECO-Aveiro Institute of Materials, UIDB/50011/2020, UIDP/50011/2020 & LA/P/0006/2020, financed by national funds through the FCT/MEC (PIDDAC) is gratefully acknowledged.

Conflict of Interests

The authors declare no conflict of interest.

Data Availability Statement

The data that support the findings of this study are available in the supplementary material of this article.

Keywords: contorted aromatics · distorted aromatics · nonplanar aromatics · polycyclic aromatic hydrocarbons · twisted aromatics · @KokeLab @ManuelMelleLab and co-workers describe the synthesis of a new series of twisted pyrene-fused azaacenes @POLYMAT_BERC @ikerbasque @ehuscientia @ciceco_ua

[1] M. A. Petrukhina, L. T. Scott, H. W. Kroto, *Fragments of Fullerenes and Carbon Nanotubes: Designed Synthesis, Unusual Reactions, and Coordination Chemistry*, Wiley, **2011**.
[2] M. Ball, Y. Zhong, Y. Wu, C. Schenck, F. Ng, M. Steigerwald, S. Xiao, C. Nuckolls, *Acc. Chem. Res.* **2015**, *48*, 267–276.
[3] Y. Segawa, A. Yagi, K. Matsui, K. Itami, *Angew. Chem. Int. Ed.* **2016**, *55*, 5136–5158.
[4] S. H. Pun, Q. Miao, *Acc. Chem. Res.* **2018**, *51*, 1630–1642.
[5] M. A. Majewski, M. Stępień, *Angew. Chem. Int. Ed.* **2019**, *58*, 86–116.
[6] R. A. Pascal, *Chem. Rev.* **2006**, *106*, 4809–4819.
[7] A. Bedi, O. Gidron, *Acc. Chem. Res.* **2019**, *52*, 2482–2490.
[8] Y. Shen, C.-F. Chen, *Chem. Rev.* **2012**, *112*, 1463–1535.
[9] M. Gingras, *Chem. Soc. Rev.* **2013**, *42*, 1051–1095.
[10] M. Rickhaus, M. Mayor, M. Juríček, *Chem. Soc. Rev.* **2016**, *45*, 1542–1556.
[11] A. Mateo-Alonso, *Eur. J. Org. Chem.* **2017**, *2017*, 7006–7011.
[12] R. A. Pascal Jr., *Chem. Rev.* **2006**, *106*, 4809–4819.
[13] M. Rickhaus, M. Mayor, M. Juríček, *Chem. Soc. Rev.* **2016**, *45*, 1542–1556.
[14] M. Rickhaus, M. Mayor, M. Juríček, *Chem. Soc. Rev.* **2017**, *46*, 1643–1660.
[15] J. M. Fernandez-Garcia, P. J. Evans, S. Filippone, M. A. Herranz, N. Martin, *Acc. Chem. Res.* **2019**, *52*, 1565–1574.
[16] I. G. Stara, I. Stary, *Acc. Chem. Res.* **2020**, *53*, 144–158.
[17] D. Cortizo-Lacalle, A. Pertegás, L. Martínez-Sarti, M. Melle-Franco, H. J. Bolink, A. Mateo-Alonso, *J. Mater. Chem. C* **2015**, *3*, 9170–9174.
[18] A. B. Marco, D. Cortizo-Lacalle, I. Perez-Miqueo, G. Valenti, A. Boni, J. Plas, K. Strutynski, S. De Feyter, F. Paolucci, M. Montes, A. N. Khlobystov, M. Melle-Franco, A. Mateo-Alonso, *Angew. Chem. Int. Ed.* **2017**, *56*, 6946–6951.
[19] J. Mateos-Martín, M. Carini, M. Melle-Franco, A. Mateo-Alonso, *Chem. Commun.* **2020**, *56*, 11457–11460.
[20] Z. Zhang, Q. Zhang, *Mater. Chem. Front.* **2020**.
[21] J. Li, S. Chen, Z. Wang, Q. Zhang, *Chem. Rec.* **2016**, *16*, 1518–1530.
[22] A. Mateo-Alonso, *Chem. Soc. Rev.* **2014**, *43*, 6311–6324.
[23] J. Li, Y. Zhao, J. Lu, G. Li, J. Zhang, Y. Zhao, X. Sun, Q. Zhang, *J. Org. Chem.* **2015**, *80*, 109–113.
[24] D. Rodriguez-Lojo, D. Perez, D. Pena, E. Guitian, *Chem. Commun.* **2015**, *51*, 5418–5420.
[25] W. Chen, X. Li, G. Long, Y. Li, R. Ganguly, M. Zhang, N. Aratani, H. Yamada, M. Liu, Q. Zhang, *Angew. Chem.* **2018**, *130*, 13743–13747.
[26] S. More, S. Choudhary, A. Higelin, I. Krossing, M. Melle-Franco, A. Mateo-Alonso, *Chem. Commun.* **2014**, *50*, 1976–1979.
[27] M. Martinez-Abadia, G. Antonicelli, E. Zuccatti, A. Atxabal, M. Melle-Franco, L. E. Hueso, A. Mateo-Alonso, *Org. Lett.* **2017**, *19*, 1718–1721.
[28] W. Fan, T. Winands, N. L. Doltsinis, Y. Li, Z. Wang, *Angew. Chem. Int. Ed.* **2017**, *56*, 15373–15377.
[29] J. Hu, D. Zhang, F. W. Harris, *J. Org. Chem.* **2005**, *70*, 707–708.
[30] D. Cortizo-Lacalle, J. P. Mora-Fuentes, K. Strutynski, A. Saeki, M. Melle-Franco, A. Mateo-Alonso, *Angew. Chem. Int. Ed.* **2018**, *57*, 703–708.
[31] D. Cortizo-Lacalle, C. Gozalvez, M. Melle-Franco, A. Mateo-Alonso, *Nanoscale* **2018**, *10*, 11297–11301.
[32] J. P. Mora-Fuentes, A. Riaño, D. Cortizo-Lacalle, A. Saeki, M. Melle-Franco, A. Mateo-Alonso, *Angew. Chem. Int. Ed.* **2019**, *58*, 552–556.
[33] Z. Wang, P. Gu, G. Liu, H. Yao, Y. Wu, Y. Li, G. Rakesh, J. Zhu, H. Fu, Q. Zhang, *Chem. Commun.* **2017**, *53*, 7772–7775.
[34] H. Sun, X. Guo, A. Facchetti, *Chem.* **2020**, *6*, 1310–1326.
[35] A. M. Brouwer, *Pure Appl. Chem.* **2011**, *83*, 2213–2228.

Manuscript received: June 23, 2023
Accepted manuscript online: September 8, 2023
Version of record online: October 25, 2023